Heliyon 10 (2024) e23739

Contents lists available at ScienceDirect

Heliyon

journal homepage: www.cell.com/heliyon

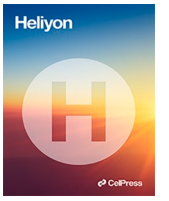

ERRα regulates synaptic transmission through reactive oxygen species in hippocampal neurons

De-Mei Xu, Zhi-Juan Zhang, Hao-Kun Guo, Guo-Jun Chen **, Yuan-Lin Ma *

Department of Neurology, The First Affiliated Hospital of Chongqing Medical University, Chongqing Key Laboratory of Neurology, 1 Youyi Road, Chongqing 400016, China

ARTICLE INFO

Keywords:
ERRα
ROS
Dendritic spines
Synaptic transmission
PBN

ABSTRACT

Reactive oxygen species (ROS) play multiple roles in synaptic transmission, and estrogen-related receptor α (ERRα) is involved in regulating ROS production. The purpose of our study was to explore the underlying effect of ERRα on ROS production, neurite formation and synaptic transmission. Our results revealed that knocking down ERRα expression affected the formation of neuronal neurites and dendritic spines, which are the basic structures of synaptic transmission and play important roles in learning, memory and neuronal plasticity; moreover, the amplitude and frequency of miniature excitatory postsynaptic currents (mEPSCs) and miniature inhibitory postsynaptic currents (mIPSCs) were decreased. These abnormalities were reversed by overexpression of human ERRα. Additionally, we also found that knocking down ERRα expression increased intracellular ROS levels in neurons. ROS inhibitor PBN rescued the changes in neurite formation and synaptic transmission induced by ERRα knockdown. These results indicate a new possible cellular mechanism by which ERRα affects intracellular ROS levels, which in turn regulate neurite and dendritic spine formation and synaptic transmission.

1. Introduction

Oxidative stress is a state of disrupted redox signaling, reactive oxygen species (ROS) overproduction and oxidative cell damage, which induces numerous brain pathologies, including Alzheimer's disease and epilepsy. Neurons generate a large amount of energy via oxidative phosphorylation in mitochondria [1] and therefore need a sufficient supply of oxygen and interconnected redox-dependent metabolic pathways [2]. This processe is accompanied by the generation of large amount of ROS [3,4]. Oxidative stress impairs synaptic transmission and plasticity, which leads to learning and memory deficits [5].

Estrogen-related receptor α (ERRα, NR3B1), which is an orphan member of the nuclear receptor superfamily and a master regulator of cellular energy metabolism [6], reduces ROS production by targeting ROS sensors [7–9]. Our previous study showed that ERRα plays an important role in Alzheimer's disease (AD) pathology by attenuating both amyloidogenesis and Tau phosphorylation [10]. Interestingly, recent evidence suggests that changes in the morphology of neuronal dendrites and synapses and dysfunction of dendritic spines are critical features in the pathogenesis of AD [11–14]. The underlying relationships between these biological phenomena are not clear.

The aim of this study was to identify the effects of ERRα on neuron formation, spine density, and synaptic transmission via ROS

* Corresponding author.
** Corresponding author.
E-mail addresses: woodchen2015@163.com (G.-J. Chen), mayuanlin2005@163.com (Y.-L. Ma).

https://doi.org/10.1016/j.heliyon.2023.e23739
Received 27 July 2023; Received in revised form 23 November 2023; Accepted 12 December 2023
Available online 15 December 2023

production. Our results show that knocking down ERRα expression increases the generation of ROS, leading to decreased neurite and spine density. These phenomena eventually result in changes in neuronal excitability and inhibition, which likely contributes to the pathological processes of synaptic transmission-related diseases, such as epilepsy and AD.

2. Materials and methods

2.1. Antibodies, reagents and western blotting

Phenyl-*N*-*tert*-butylnitrone (PBN) (B7263-1G) was purchased from Sigma Aldrich. Protein extracts from neurons and HEK-293 cells were collected for Western blot analysis. Each lane was loaded 10 μg total protein, and the samples were separated by 10 % SDS−PAGE gels and transferred to 0.45 μm polyvinylidene difluoride membranes (Millipore, IPVH00010). The membranes were blocked with protein-free rapid blocking buffer (EpiZyme cat #: PS108P) for 20 min at room temperature, followed by incubation with mouse anti-Flag (Sigma-Aldrich, cat: F1804, 1:1000), rabbit anti-ERRα (GeneTex, cat: GTX108166, 1:1000), mouse anti-GAPDH (Proteintech, cat: 60004-1-Ig) antibodies overnight at 4 °C. The membranes were washed 3 times and then incubated with a horseradish peroxidase (HRP)–conjugated anti-mouse or anti-rabbit secondary antibody (Proteintech, cat: SA00001-1 or SA00001-2) for 1 h at room temperature. Immunoreactive bands were visualized using a Western blotting detection kit (ZEN BIO, cat:17047) according to the manufacturer's recommendation. The gray density of the blotting brand was analyzed with the software (Fusion-FX5), and was normalized to the density of the GAPDH.

2.2. Primary neuron culture, plasmid and virus transfection

Brains were harvested from neonatal pups (P0–P1) of C57BL/6 mice, and hippocampal tissues were dissected and placed in pre-chilled HBSS solution. Then, the tissues were cut into approximately 1 mm^3 blocks with ophthalmic scissors and digested in 2–4 ml 0.125 % trypsin at 37 °C for 10 min (with gentle shaking every 2 min). Then, an equal volume of culture medium (DMEM supplemented with 20 % FBS) was added to the samples, and the samples were gently resuspended into single-cell suspensions, filtered and centrifuged at 1000 rpm for 5 min. Next, the supernatant was removed, and the cells were resuspended with culture medium. Approximately 1 million cells were seeded in a 3.5 cm dish, and after 4 h, the medium was replaced with 3 ml maintenance medium (neurobasal medium supplemented with 2 % B27, 1 % L-Glu, 1 % penicillin–streptomycin). Half of the medium was replaced with fresh maintenance medium every two days. The day of culture was considered DIV0; on DIV4 or DIV7, the neurons were transfected with control vector and ERRa shRNA mixed with Venus-GFP vector at a ratio of 3:1 (3 μg:1 μg), using calcium phosphate precipitation method; for the rescue experiments, ERRa shRNA was mixed with a human ERRa overexpression plasmid and Venus-GFP vector at a 6:3:1 ratio (3 μg:1.5 μg:0.5 μg), using calcium phosphate precipitation method. The mouse ERRa shRNA-#2 target sequence is : 5′-AGCCAGTCCTGACAGTCCAAA-3′. For shRNA knockdown efficiency experiment, the mouse Flag-ERRa over-expression plasmid was co-transfected with the shRNA plasmid (3 μg:1 μg) in HEK-293 cell line under the manufacturer's recommended protocol of Lipofectamine 3000 (Invitrogen, USA). At least three independent cultures were performed for each experiment. All lentivirus used in this experiment were from Obio Technology Co. Ltd (Shanghai, China).

2.3. Immunofluorescence staining and morphological analysis

On DIV10 or DIV14, transfected neurons were fixed in 4 % PFA at 37 °C for 30 min. Then, the fixed neurons were washed three times with PBS for 5 min and subjected to immunofluorescence staining. The neurons were permeabilized and blocked in PBS supplemented with 5 % goat serum, 3 % BSA and 0.3 % Triton X-100 for 30 min at room temperature and then incubated with an anti-GFP antibody (Invitrogen, USA) at 4 °C overnight. The neurons were washed three times with PBS for 5 min, followed by incubation with secondary antibodies (Alexa 488-conjugated goat anti-rabbit, Invitrogen, USA) for 1 h at room temperature. Confocal images were acquired with a Leica SP8. The number of neurites was counted on DIV10, while the density of spines (numbers of spines branching from dendrites per 10 μm) was analyzed on DIV14. The complexity of the neuron, such as dendrite branching, was analyzed using the Sholl analysis, calculating the intersections per circle with an interval of 25 μm for the circles (25 μm,50 μm,75 μm,100 μm, 125 μm, 150 μm), while the density of spines (numbers of spines branching from dendrites per 10 μm) from primary or secondary branching of the dendrite was analyzed on DIV14.

2.4. Electrophysiology

Whole-cell recordings were performed on neurons (DIV 14–18) cultured on coverslips. The recording electrodes were filled with an intracellular solution, which contained 120 mM potassium-gluconate, 10 mM KCl, 5 mM NaCl, 1 mM $CaCl_2$, 2 mM $MgCl_2$, 1 mM EGTA, 10 mM HEPES, 2 mM Mg-ATP, and 1 mM Na_2GTP and was adjusted to pH 7.3 with KOH. The extracellular solution contained 140 mM NaCl, 5 mM KCl, 1.8 mM $CaCl_2$, 1 mM $MgCl_2$, 10 mM HEPES, and 10 mM D-glucose and was adjusted to pH 7.4 with NaOH. Then, 100 μM picrotoxin and 1 μM tetrodotoxin were added to the extracellular solutions to block GABA-A receptor–mediated currents and sodium channels, which allowed the recording of miniature excitatory postsynaptic currents (mEPSCs). For mIPSCs recording, glass microelectrodes were filled with the intracellular solution containing: 100 mM CsCl, 10 mM HEPES, 1 mM $MgCl_2{\cdot}6H_2O$, 1 mM EGTA, 30 mM *N*-methyl-*d*-glucamine, 5 mM MgATP, 12 mM phosphocreatine, and 0.5 mM Na_2GTP. To isolate the miniature inhibitory postsynaptic currents (mIPSCs), 10 μM DNQX, 50 μM 2-amino-5-phosphonovaleric acid, and 1 μM TTX were added to the extracellular

solutions. The neurons were at a holding potential of −70 mV during voltage clamping to record mEPSCs and mIPSCs. Current signals were filtered at 1 kHz and digitized at 5 kHz using a Digidata 1440 A digitizer. The current traces were recorded on a computer using Clampex 10.3. The frequencies and amplitudes of mEPSCs and mIPSC were analyzed by Clampfit 10.3 and minianalysis.

2.5. Assessment of cellular ROS production with an ROS assay kit

A ROS Assay Kit (S0033S, Beyotime, China) was used to measure the total cellular ROS levels in neurons according to the manufacturer's recommended protocol. Neurons were seeded on coverslips in 6-well plates for imaging. The medium was removed after the neurons were treated according to the experimental conditions, and the cells were incubated with 10 μM DCFH-DA for 20 min at 37 °C. The change in DCFH-DA fluorescence in the 6-well plates was measured with a confocal microscope at an excitation wavelength of 488 nm and an emission wavelength of 525 nm.

2.6. Statistical analysis

Student's *t*-test was used for upaired two-group comparing, and one-way analysis of variance (ANOVA) was used for more than two groups comparisons followed by post hoc Bonferroni test for multiple comparisons. Nonnormally distributed data were analyzed by using the Mann–Whitney *U* test or Kruskal–Wallis test for two or more group comparisons. $P < 0.05$ was considered as statistical significance.

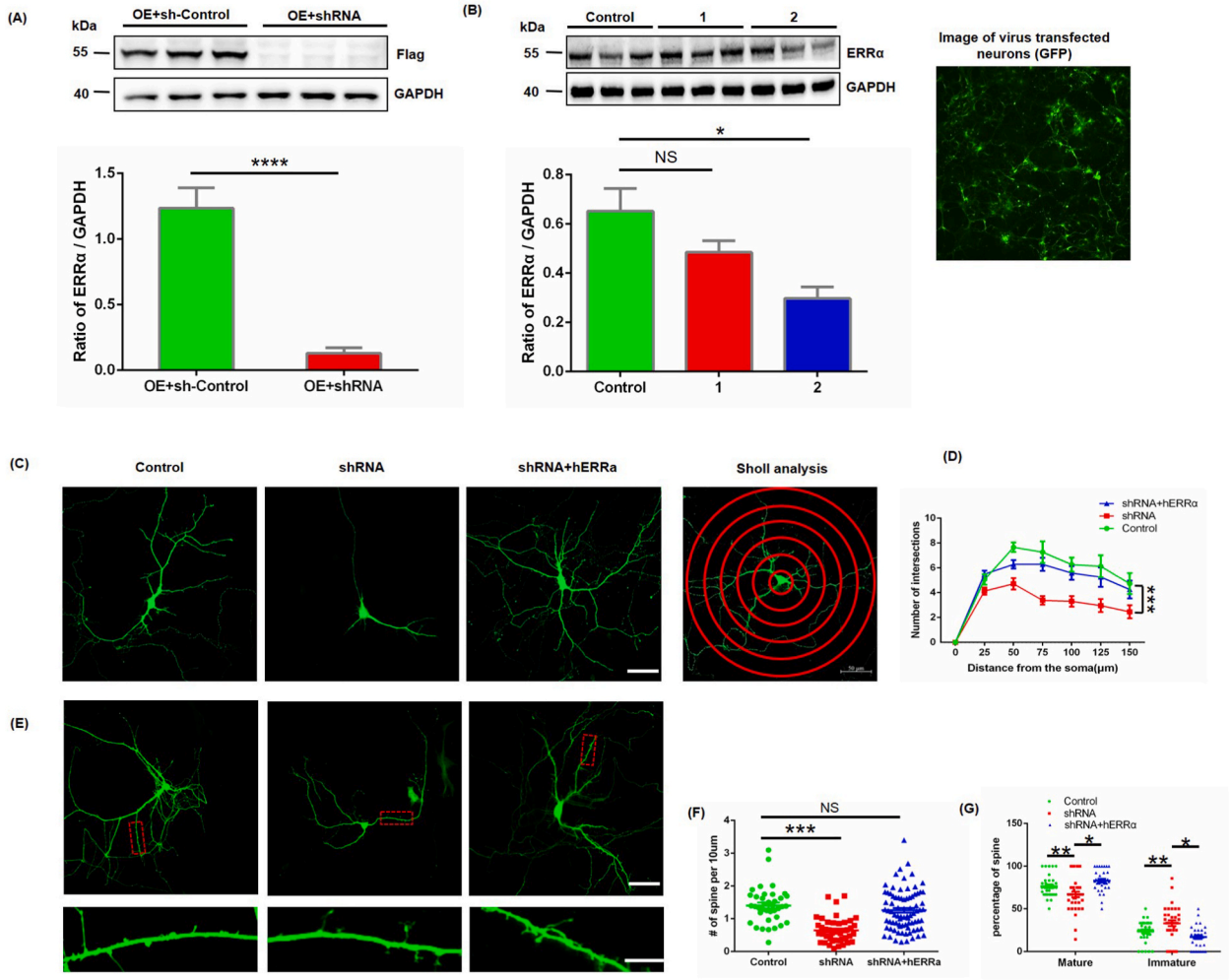

Fig. 1. ERRα affects neurite and synapse formation. Western blots showing that ERRα was efficiently knockdown in plasmid-transfected HEK-293 cells (A) and lentivirus-infected neurons (B). Representative confocal images of neurons (C) (scale bar = 50 μm) and the spine density (E) (scale bar = 20 μm). Quantification of neurite complex using Sholl analysis (D) (control: n = 13, shRNA: n = 13, shRNA + hERRα: n = 12) and spine density (F) (control: n = 38, shRNA: n = 45, shRNA + hERRα: n = 81). The percentage of mature and immature spine (G) (n = 35). The data were analyzed by one-way ANOVA with post hoc test. All the data are presented as the mean ± S.E.M., *, $P < 0.05$; **, $P < 0.01$; ***, $P < 0.001$.

3. Results

3.1. ERRα knockdown inhibited neurite and synapse formation

Many nervous system diseases, such as autism and schizophrenia, are characterized by abnormalities in neuron morphology

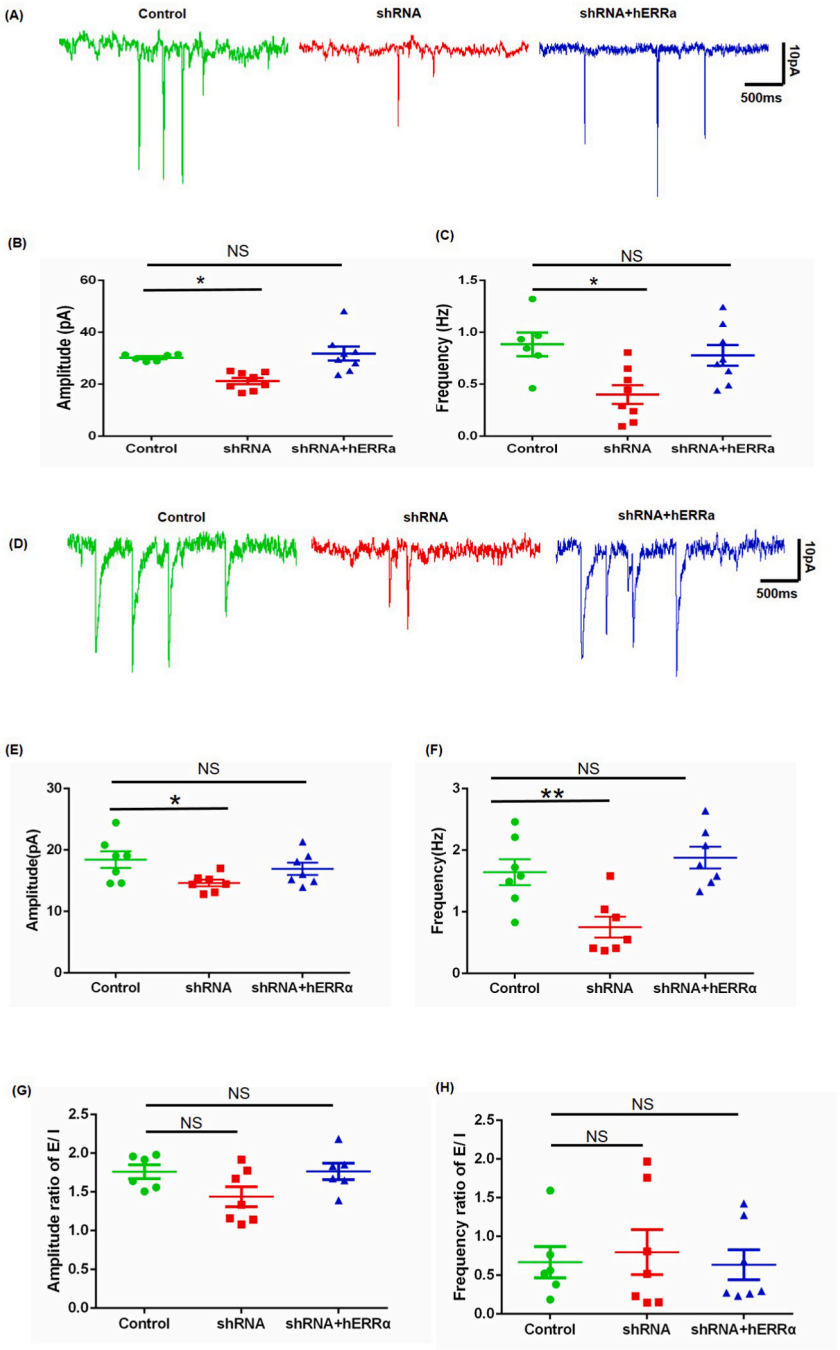

Fig. 2. Knockdown of ERRα decreases neuronal synaptic transmission. Representative traces of whole-cell voltage-clamp recordings of mEPSCs (A) and mIPSCs (D), quantitative analysis of mEPSC amplitude (B) and frequency (C) (control: n = 6, shRNA: n = 8, shRNA + hERRα: n = 8), and quantitative analysis of mIPSCs amplitude (E) and frequency (F) (n = 7). The ratio of mEPSC/mIPSC (E/I) amplitude (G) and frequency (H) (control: n = 6, shRNA: n = 7, shRNA + hERRα: n = 7). The data were analyzed by one-way ANOVA with post hoc test. All the data are presented as the mean ± S.E.M. *, $P < 0.05$; **, $P < 0.01$.

[15–18]. In addition, our previous study showed that ERRα affects AD, which is also characterized by changes in the morphology of neuronal dendrites and synapses [10]. ERRα is also required for the expression of the PGC-1α gene [19,20], which is a critical gene that promotes the expression of genes involved in synchronous neurotransmitter release, axonal integrity, and metabolism. We thus reasoned that ERRα affected AD via its protective effect on the morphology of neurons. We aimed to investigate whether ERRα plays a role in neurite and synapse formation. In lentivirus-infected neurons, there was no knockdown efficiency in sequence-#1, but about 60 % reduction in sequence #2. Therefore, we selected sequence-#2 for subsequent experiments (Fig. 1B). We also co-transfected the mouse Flag-ERRa over-expression plasmid with the shRNA-#2 plasmid (3 μg:1 μg) in HEK-293 cell line, the efficiency of ERRa knockdown was confirmed by western blotting, which showed about 80 % reduction in the expression of Flag-ERRa (Fig. 1A). For complexity of neuronal dendrites analysis, we transfected neurons with control, shRNA-ERRα and shRNA-ERRa mixed with hERRa plasmids on DIV4 using calcium phosphate precipitation method. On DIV10, the neurons were fixed and stained, and confocal images were acquired and analyzed by Sholl analysis. For spine analysis, the plasmids were transfected on DIV7, and the neurons were fixed on DIV14. The complexity of neuronal dendrites, dendritic spines and mature dendritic spines in the shRNA group were significantly reduced compared with those in the control group, while shRNA + hERRα reversed these morphological alterations in neurons (Fig. 1C–G). These results suggest that ERRα affects neuronal development.

3.2. *Silencing of ERRα reduced both excitatory and inhibitory neurotransmission*

Dendritic spines are the critical site of synaptic transmission in the central nervous system and influence signaling mechanisms at individual synapses [21,22]. Pink−/− neurons showed significant reductions in spine density and mEPSCs frequency [23]. To further examine the effect of ERRα on neuronal synaptic transmission, we used whole-cell voltage-clamp recording to measure the amplitudes

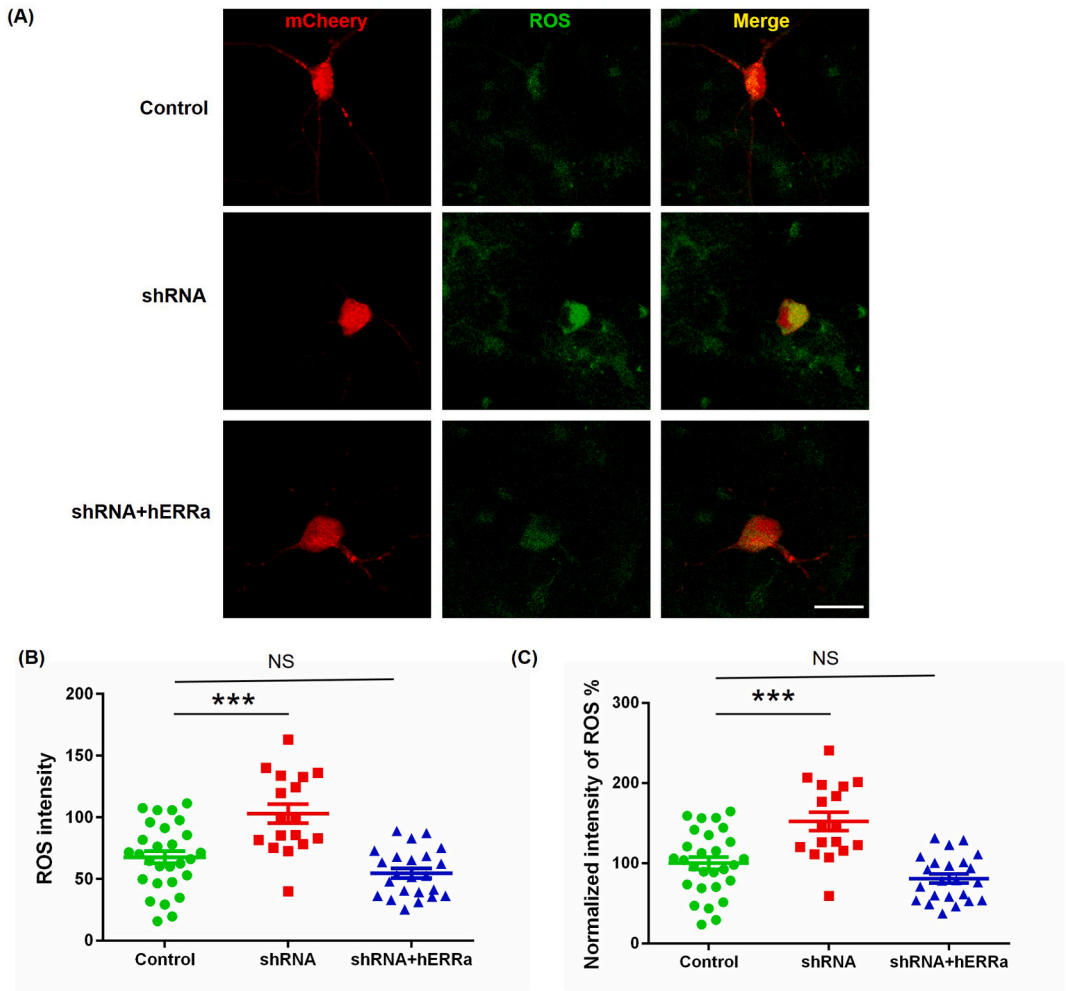

Fig. 3. Knocking down ERRα expression increases the level of ROS in neurons. Representative DCFH-DA assay images of neurons (A), scale bar = 20 μm. Quantification of ROS generation in neurons by DCFH-DA assay (B) and (C) (control: n = 28, shRNA: n = 17, shRNA + hERRα: n = 23). The data were analyzed by one-way ANOVA with post hoc test. All the data are presented as the mean ± S.E.M. ***, $P < 0.001$.

and frequencies of mEPSCs and mIPSCs in neurons (DIV 14–18). mEPSCs were recorded in the presence of an extracellular solution containing 100 μM picrotoxin and 1 μM tetrodotoxin. For mIPSC recording, 10 μM DNQX, 50 μM DL-APV and 1 μM tetrodotoxin were added to the extracellular solution. The membrane potentials were held at −70 mV. The results showed that the amplitudes and frequencies of mEPSCs and mIPSCs in the shRNA group were significantly decreased compared with those in the control group, whereas these properties were not altered in the shRNA + hERRα group (Fig. 2A–F). Interestingly, there was no difference in the ratio of mEPSC/mIPSC (E/I) amplitude and frequency (Fig. 2G and H). The data described above indicated that ERRα may regulate neuronal excitability and inhibition.

3.3. Both excitatory and inhibitory neurotransmission were inhibited by ROS

We next examined the mechanisms by which ERRα regulates neurotransmission. ROS were found to negatively regulate the dendritic arbor size of the motoneurons in Drosophila embryos and larvae [24]. We examined whether ERRα affects the production of ROS in neurons. On DIV4, in addition to the mCherry plasmids, the neurons were cotransfected with control, shRNA-ERRα and shRNA-ERRa mixed with hERRa plasmids; on DIV14, we used an ROS Assay Kit to measure the ROS levels in the neurons. The shRNA group showed increased levels of ROS, while there was no significant difference between the control group and the shRNA + hERRα

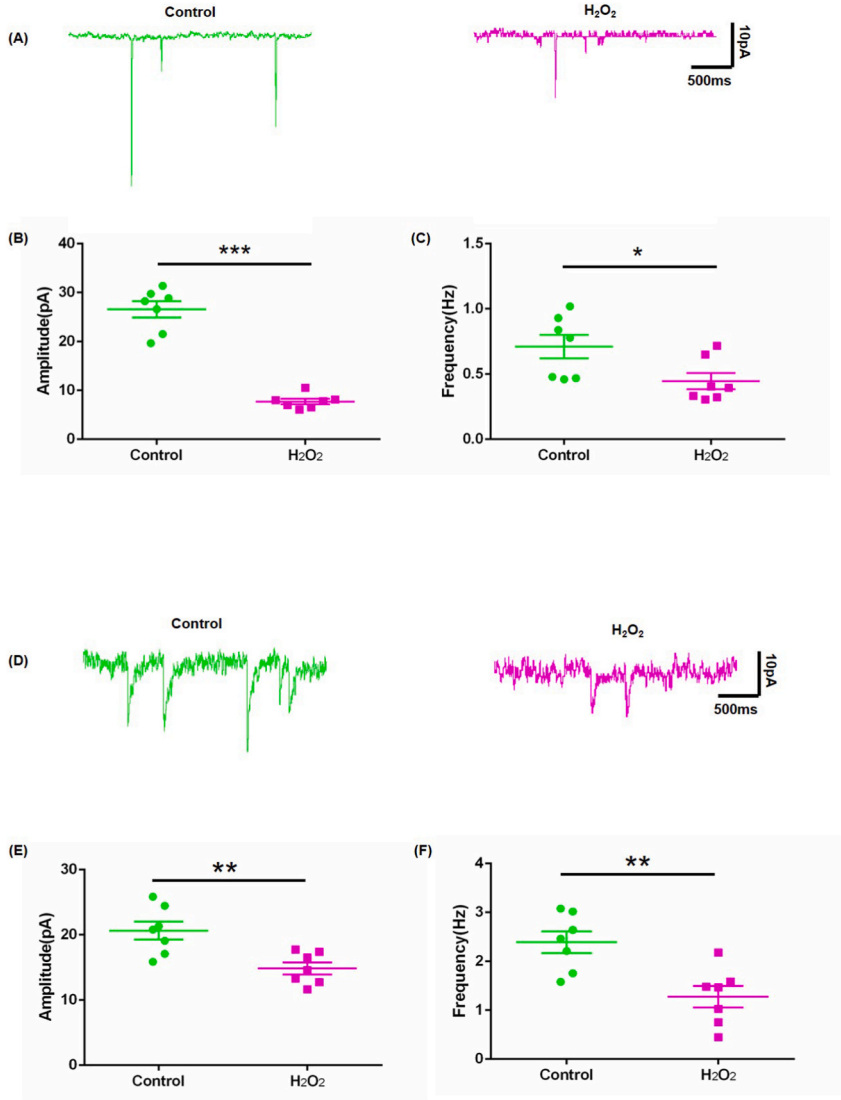

Fig. 4. ROS alter synaptic transmission. Neurons were pretreated with H_2O_2 (30 μM) for 30 min and then subjected to whole-cell voltage-clamp recording. Representative traces of whole-cell voltage-clamp recordings of mEPSCs (A) and mIPSCs (D) and quantitative analysis of mEPSC amplitude (B) and frequency (C) and mIPSC amplitude (E) and frequency (F). The data were analyzed by unpaired *t*-test. All data are presented as the mean ± S.E.M. *, $P < 0.05$; **, $P < 0.01$; ***, $P < 0.001$, ($n = 7$).

group (Fig. 3A–C). These data indicated that ERRα affected ROS production.

We next tested whether ROS affected synaptic transmission. For this purpose, whole-cell voltage-clamp recording in neurons (DIV 14–18) was performed. The amplitudes and frequencies of mEPSCs and mIPSCs were significant decreased when the neurons were pretreated with H_2O_2 (Fig. 4A–F) [25], suggested that ROS reduced synaptic transmission.

3.4. ROS scavenger PBN rescued the effect of ERRα on neurite formation and synaptic transmission

To assess the role of ROS in ERRα-mediated synaptic alterations, neurons were treated with ROS inhibitor phenyl-N-tert-butylnitrone (PBN). The results showed that PBN treatment rescued the reduction in the complexity of neuronal dendrites, dendritic spines and mature dendritic spines caused by shRNA (Fig. 5A–D). To further examine the functional alterations generated by shRNA followed by rescue with PBN, we recorded mEPSCs and mIPSCs in neurons (DIV 14–18). Consistent with the morphological results, we found that PBN treatment rescued the changes in mEPSC and mIPSC amplitudes and frequencies induced by shRNA (Fig. 5E–J). Therefore, the shRNA-induced alterations in neuronal dendrites and dendritic spines were reflected as functional alterations at synapses. Collectively, these results indicate that ERRα regulated the morphology and function of synapses by affecting the production of ROS. Oxidative stress is an important triggering factor for migraine [26]. Quercetin has antimigraine effects through its antioxidant activity [27]. Therefore, intervening with ERRα expression may be a new strategy for preventing and treating migraine.

4. Discussion

A previous study found that ERRα has a neuroprotective effect on AD [10], but the underlying mechanisms remain unknown. The

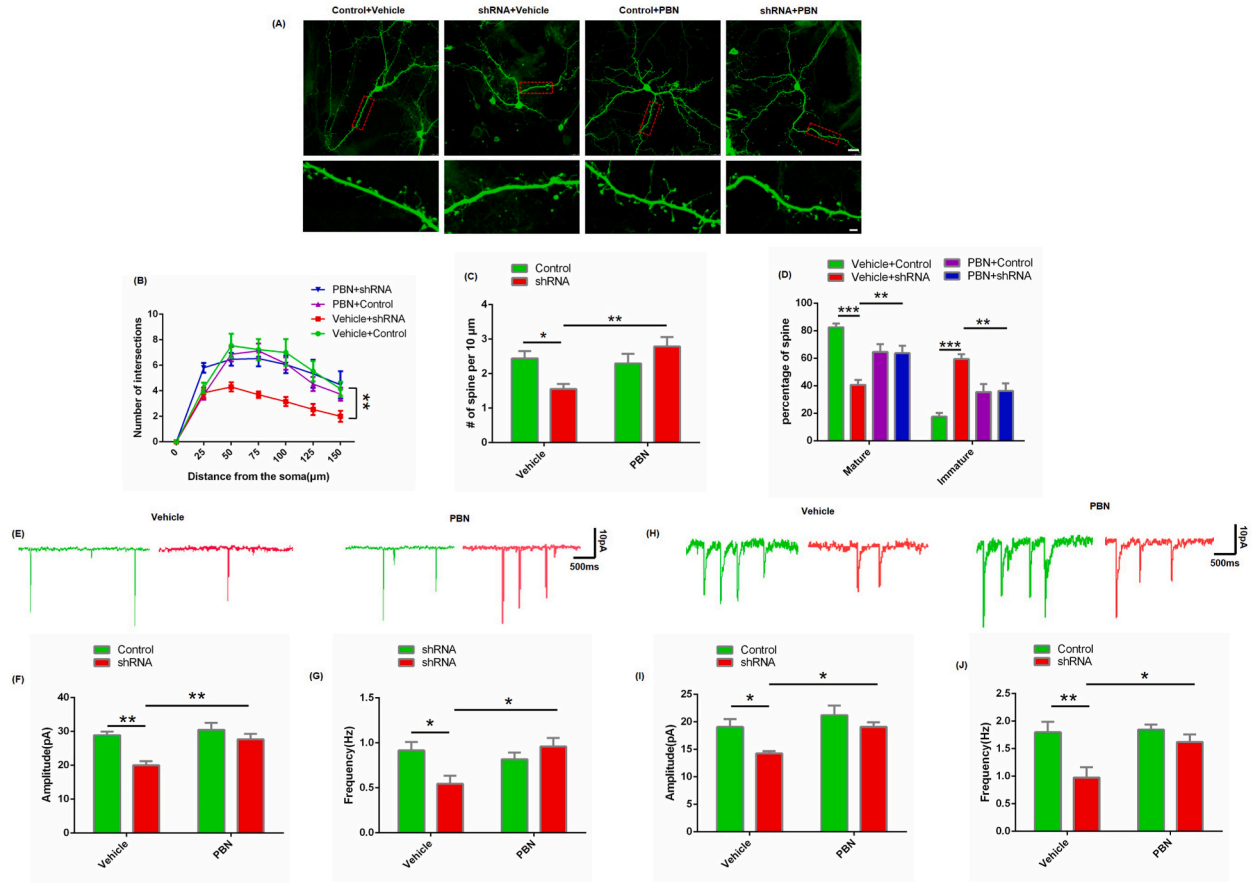

Fig. 5. The role of ROS in ERRα-mediated synaptic alterations. Neurons were treated with PBN (500 μM) after plasmid transfection on DIV2. Representative confocal images of the neuron and spine density. Scale bar (upper) = 10 μm; scale bar (lower) = 3 μm (A). Quantification of neuron complexity using Sholl analysis(B) (control + vehicle: n = 11, shRNA + vehicle: n = 11, control + PBN: n = 11, shRNA + PBN: n = 13) and spine density (C). The percentage of mature and immature spine (D). Representative traces of whole-cell voltage-clamp recordings of mEPSCs (E) and mIPSCs (H) and quantitative analysis of mEPSC amplitude (F) and frequency (G) and mIPSC amplitude (I) and frequency (J). The data were analyzed by two-way ANOVA followed by a post hoc test. All data are presented as the mean ± S.E.M. *, $P < 0.05$; **, $P < 0.01$; ***, $P < 0.001$, (n = 25).

main clinical manifestations of AD are impaired learning and memory, which are closely linked to the structure, function, and plasticity of synapses [28]. The loss of ERRα expression disrupts the synaptic function of ventral striatal neurons without affecting spine density in female mice [29]. However, the role of ERRα in hippocampal neuronal function is unclear. In the present study, we found that ERRα altered not only spine density but also synaptic transmission.

Alterations in the frequency of mEPSCs and mIPSCs are typically associated with changes to either the postsynaptic dendritic spine density or the probability of presynaptic vesicle release [30,31]. We conducted morphological and electrophysiological analyses. As the neuronal spine density was significantly different between the shRNA-ERRα and control groups, the decreased frequency of mEPSCs and mIPSCs may have been the result of reduced spine density. The current study was not designed to measure the number and size of vesicles, which determine the release rate of vesicles. The concentration of neurotransmitters per vesicle is higher in neurons, and each vesicle is able to release more glutamate into the synaptic cleft. Therefore, increased synaptic transmission can be observed [32]. In the future, further assessment of presynaptic vesicles will be useful to explore these possibilities. Altered amplitudes of mEPSCs and mIPSCs are typically associated with postsynaptic alterations, which is consistent with a postsynaptic mechanism. Neurons transfected with shRNA-ERRα exhibited significantly decreased amplitudes.

Large amounts of ROS are produced in the neurons of the brain, and the balance of ROS is maintained by a network of antioxidants. Excessive levels of ROS lead to decreased cognitive function and excitatory and inhibitory synapse densities in neurons [33,34]. We have shown that the level of ROS was significantly increased and dendritic spine density was decreased in neurons transfected with shRNA-ERRα. The oxidative stress inhibitor PBN rescued the changes in synaptic morphology and function induced by shRNA-ERRα. These results were consistent with those of a previous study.

In summary, our study suggests that knockdown of ERRα expression leads to the generation of ROS and modulates dendritic spine densities in hippocampal neurons. Eventually, the frequency and amplitude of mEPSCs and mIPSCs were changed. Our results provide a new molecular mechanism underlying the role of ERRα in neuronal function, and these results may be beneficial for the treatment of synaptic transmission-related neurological diseases.

Ethics approval

This study was reviewed and approved by Commission of Chongqing Medical University for Ethics of Experiments on Animals with the approval number: IACUC-CQMU-2023-0146.

Funding

This work was supported by the National Natural Science Foundation of China (grant numbers:82101517, 81901332).

Data availability statement

Question 1#, Has data associated with your study been deposited into a publicly available repository?
Response 1#, Yes.
Quetion2#, Please provide the name of the repository and the accession number here.
Response 2#, xu, demei (2023), “The raw data of ERRα”, Mendeley Data, V1, doi: 10.17632/gkdm6z9c2y.1.

Additional information

No additional information is available for this paper.

CRediT authorship contribution statement

De-Mei Xu: Conceptualization, Data curation, Formal analysis, Funding acquisition, Investigation, Methodology, Project administration, Validation, Writing - original draft, Writing - review & editing. **Zhi-Juan Zhang:** Data curation, Formal analysis, Methodology. **Hao-Kun Guo:** Data curation, Investigation, Methodology. **Guo-Jun Chen:** Conceptualization, Project administration, Supervision, Writing - review & editing. **Yuan-Lin Ma:** Conceptualization, Data curation, Formal analysis, Funding acquisition, Investigation, Methodology, Project administration, Supervision, Writing - original draft, Writing - review & editing.

Declaration of competing interest

The authors declare the following financial interests/personal relationships which may be considered as potential competing interests:Yuanlin Ma reports financial support was provided by National Natural Science Foundation of China. Demei Xu reports financial support was provided by National Natural Science Foundation of China. If there are other authors, they declare that they have no known competing financial interests or personal relationships that could have appeared to influence the work reported in this paper.

Appendix A. Supplementary data

Supplementary data to this article can be found online at https://doi.org/10.1016/j.heliyon.2023.e23739.

References

[1] C.N. Hall, M.C. Klein-Flugge, C. Howarth, D. Attwell, Oxidative phosphorylation, not glycolysis, powers presynaptic and postsynaptic mechanisms underlying brain information processing, J. Neurosci. 32 (26) (2012) 8940–8951.
[2] S. Ozugur, L. Kunz, H. Straka, Relationship between oxygen consumption and neuronal activity in a defined neural circuit, BMC Biol. 18 (1) (2020) 76.
[3] C. Quijano, M. Trujillo, L. Castro, A. Trostchansky, Interplay between oxidant species and energy metabolism, Redox Biol. 8 (2016) 28–42.
[4] C.C. Winterbourn, Reconciling the chemistry and biology of reactive oxygen species, Nat. Chem. Biol. 4 (5) (2008) 278–286.
[5] A. Kumar, B. Yegla, T.C. Foster, Redox signaling in neurotransmission and cognition during aging, Antioxidants Redox Signal. 28 (18) (2018) 1724–1745.
[6] V. Giguere, N. Yang, P. Segui, R.M. Evans, Identification of a new class of steroid hormone receptors, Nature 331 (6151) (1988) 91–94.
[7] S.M. Rangwala, X. Li, L. Lindsley, X. Wang, S. Shaughnessy, T.G. Daniels, J. Szustakowski, N.R. Nirmala, Z. Wu, S.C. Stevenson, Estrogen-related receptor alpha is essential for the expression of antioxidant protection genes and mitochondrial function, Biochem. Biophys. Res. Commun. 357 (1) (2007) 231–236.
[8] P. Chen, H. Wang, Z. Duan, J.X. Zou, H. Chen, W. He, J. Wang, Estrogen-related receptor alpha confers methotrexate resistance via attenuation of reactive oxygen species production and P53 mediated apoptosis in osteosarcoma cells, BioMed Res. Int. 2014 (2014), 616025.
[9] M. Vernier, C.R. Dufour, S. McGuirk, C. Scholtes, X. Li, G. Bourmeau, H. Kuasne, M. Park, J. St-Pierre, E. Audet-Walsh, V. Giguere, Estrogen-related receptors are targetable ROS sensors, Genes Dev. 34 (7–8) (2020) 544–559.
[10] Y. Tang, Z. Min, X.J. Xiang, L. Liu, Y.L. Ma, B.L. Zhu, L. Song, J. Tang, X.J. Deng, Z. Yan, G.J. Chen, Estrogen-related receptor alpha is involved in Alzheimer's disease-like pathology, Exp. Neurol. 305 (2018) 89–96.
[11] R.J. Bevan, T.R. Hughes, P.A. Williams, M.A. Good, B.P. Morgan, J.E. Morgan, Retinal ganglion cell degeneration correlates with hippocampal spine loss in experimental Alzheimer's disease, Acta Neuropathol Commun 8 (1) (2020) 216.
[12] E.E. Reza-Zaldivar, M.A. Hernandez-Sapiens, B. Minjarez, U. Gomez-Pinedo, V.J. Sanchez-Gonzalez, A.L. Marquez-Aguirre, A.A. Canales-Aguirre, Dendritic spine and synaptic plasticity in alzheimer's disease: a focus on MicroRNA, Front. Cell Dev. Biol. 8 (2020) 255.
[13] J. Ma, Y. Gao, W. Tang, W. Huang, Y. Tang, Fluoxetine protects against dendritic spine loss in middle-aged APPswe/PSEN1dE9 double transgenic alzheimer's disease mice, Curr. Alzheimer Res. 17 (1) (2020) 93–103.
[14] H. Kim, B. Kim, H.S. Kim, J.Y. Cho, Nicotinamide attenuates the decrease in dendritic spine density in hippocampal primary neurons from 5xFAD mice, an Alzheimer's disease animal model, Mol. Brain 13 (1) (2020) 17.
[15] Z. Zhang, M. Ye, Q. Li, Y. You, H. Yu, Y. Ma, L. Mei, X. Sun, L. Wang, W. Yue, R. Li, J. Li, D. Zhang, The schizophrenia susceptibility gene OPCML regulates spine maturation and cognitive behaviors through eph-cofilin signaling, Cell Rep. 29 (1) (2019) 49–61 e7.
[16] J. Li, A. Chai, L. Wang, Y. Ma, Z. Wu, H. Yu, L. Mei, L. Lu, C. Zhang, W. Yue, L. Xu, Y. Rao, D. Zhang, Synaptic P-Rex 1 signaling regulates hippocampal long-term depression and autism-like social behavior, Proc. Natl. Acad. Sci. U. S. A. 112 (50) (2015) E6964–E6972.
[17] Z. Zhang, F. Zheng, Y. You, Y. Ma, T. Lu, W. Yue, D. Zhang, Growth arrest specific gene 7 is associated with schizophrenia and regulates neuronal migration and morphogenesis, Mol. Brain 9 (1) (2016) 54.
[18] T. Chen, Q. Wu, Y. Zhang, T. Lu, W. Yue, D. Zhang, Tcf 4 controls neuronal migration of the cerebral cortex through regulation of Bmp 7, Front. Mol. Neurosci. 9 (2016) 94.
[19] L.J. McMeekin, K.L. Joyce, L.M. Jenkins, B.M. Bohannon, K.D. Patel, A.S. Bohannon, A. Patel, S.N. Fox, M.S. Simmons, J.J. Day, A. Kralli, D.K. Crossman, R. M. Cowell, Corrigendum to "Estrogen-related receptor alpha (ERRalpha) is required for PGC-1alpha-dependent gene expression in the mouse brain", Neuroscience 479 (2021) 70–90. Neuroscience 493 (2022) 119.
[20] Q. Zhou, H. Xu, L. Yan, L. Ye, X. Zhang, B. Tan, Q. Yi, J. Tian, J. Zhu, PGC-1alpha promotes mitochondrial respiration and biogenesis during the differentiation of hiPSCs into cardiomyocytes, Genes Dis 8 (6) (2021) 891–906.
[21] J.N. Bourne, K.M. Harris, Balancing structure and function at hippocampal dendritic spines, Annu. Rev. Neurosci. 31 (2008) 47–67.
[22] K.F. Lee, C. Soares, J.C. Beique, Examining form and function of dendritic spines, Neural Plast. (2012), 704103, 2012).
[23] P.A. Otero, G. Fricklas, A. Nigam, B.N. Lizama, Z.P. Wills, J.W. Johnson, C.T. Chu, Endogenous PTEN-induced kinase 1 regulates dendritic architecture and spinogenesis, J. Neurosci. 42 (41) (2022) 7848–7860.
[24] S. Dhawan, P. Myers, D.M.D. Bailey, A.D. Ostrovsky, J.F. Evers, M. Landgraf, Reactive oxygen species mediate activity-regulated dendritic plasticity through NADPH oxidase and aquaporin regulation, Front. Cell. Neurosci. 15 (2021), 641802.
[25] X. Chen, Q. Zhang, Q. Cheng, F. Ding, Protective effect of salidroside against H2O2-induced cell apoptosis in primary culture of rat hippocampal neurons, Mol. Cell. Biochem. 332 (1–2) (2009) 85–93.
[26] J.M. Borkum, Migraine triggers and oxidative stress: a narrative review and synthesis, Headache 56 (1) (2016) 12–35.
[27] A.I. Foudah, S. Devi, M.H. Alqarni, A. Alam, M.A. Salkini, M. Kumar, H.S. Almalki, Quercetin attenuates nitroglycerin-induced migraine headaches by inhibiting oxidative stress and inflammatory mediators, Nutrients 14 (22) (2022).
[28] P. Smolen, Y. Zhang, J.H. Byrne, The right time to learn: mechanisms and optimization of spaced learning, Nat. Rev. Neurosci. 17 (2) (2016) 77–88.
[29] H. De Jesus-Cortes, Y. Lu, R.M. Anderson, M.Z. Khan, V. Nath, L. McDaniel, M. Lutter, J.J. Radley, A.A. Pieper, H. Cui, Loss of estrogen-related receptor alpha disrupts ventral-striatal synaptic function in female mice, Neuroscience 329 (2016) 66–73.
[30] S.M. Wojcik, N. Brose, Regulation of membrane fusion in synaptic excitation-secretion coupling: speed and accuracy matter, Neuron 55 (1) (2007) 11–24.
[31] C. Sala, M. Segal, Dendritic spines: the locus of structural and functional plasticity, Physiol. Rev. 94 (1) (2014) 141–188.
[32] X.S. Wu, L. Xue, R. Mohan, K. Paradiso, K.D. Gillis, L.G. Wu, The origin of quantal size variation: vesicular glutamate concentration plays a significant role, J. Neurosci. 27 (11) (2007) 3046–3056.
[33] C.A. Massaad, E. Klann, Reactive oxygen species in the regulation of synaptic plasticity and memory, Antioxidants Redox Signal. 14 (10) (2011) 2013–2054.
[34] Y. Cai, L. Yang, G. Hu, X. Chen, F. Niu, L. Yuan, H. Liu, H. Xiong, J. Arikkath, S. Buch, Regulation of morphine-induced synaptic alterations: role of oxidative stress, ER stress, and autophagy, J. Cell Biol. 215 (2) (2016) 245–258.